

Self Organized Grouping of Ears Based on Inertia Related Biometrics Using Kohonen's Feature Map

Prashanth G. K.^{*}, M. A. Jayaram, Gaddi Siddharam

Department of MCA, Siddaganga Institute of Technology, Tumkur, Karnataka, India

Abstract Classification of images based on the biometric features is a challenging problem in the field of pattern recognition and person identification. In this paper, we propose a Self Organized Feature Map (SOFM) to group ears for the purpose of person identification. A database of 605 right ear images is used to develop the recognition system. The application of SOFM permitted to differentiate four classes of ears. The features used are novel and are based on the Moment of Inertia (MI) related parameters. To elicit the parameters the ear is considered to be planar surface. Five parameters namely MI with respect to major axis and minor axis, radii of gyration (RG) with respect to major axis and minor axis, and the planar area of the ear were considered. The results show that four groups are distinct with minimum overlapping. The group characteristic has also been reported. The significance of this work is seen in decreased grouping and image retrieval time to an extent of 10% when the images in the database is organized in blocks of groups when compared to image matching and retrieval time when unorganized database is considered.

Keywords Ear biometrics, SOFM, Moment of inertia, Radii of gyration, Major axis, Minor axis

1. Introduction

Biometrics is basically identification or self verification by taking personality information that corresponds to an individual [1, 2]. Biometrics can be categorized into two types, which are behavioural and physical [3].

The human ear is becoming a popular biometric feature in recent years. It has several advantages over other biometric technologies such as iris, fingerprints, face and retinal scans. Ear is large when compared with iris and fingerprint. Further the image acquisition of human ear is very easy as it can be captured from a distance without the cooperation of an individual [6]. Human ear contains rich and stable features and it is more reliable than face as the structure of ear is not subject to change with the age and facial expressions. It has been found that no two ears are exactly the same even that of identical twins [7, 8]. Therefore, it is proved beyond doubt that the ear biometrics is a good solution for computerized human identification and verification systems. The major application of this technology is in crime investigation. Ear features have been used for many years in the forensic sciences for recognition.

A profound work of ear identification involving over 10000, ears has been documented [4]. In an experiment involving larger datasets more rigorously controlled for

relative quality of face and ear, the recognition performance was almost same when ear and face were individually considered. However, the performance shot up to 90.9% when both ear and face were considered [3]. Ear biometrics is an unexplored biometric field, but has received a growing amount of attention over the past few years. There are three modes of ear biometrics: ear photographs, ear prints obtained by pressing the ear against a flat plane, and thermograph pictures of the ear. The most common implementation of ear biometrics is via photographs for identification systems [4].

The rest of the paper is organised as follows. Section 2 elaborates on related Works; Kohonen's Feature Map is briefed in section 3. The way in which the data was acquired is explained in section 4. Moment of inertia (MI) based feature extraction is presented in section 5. The result and discussion are made in section 6, and the paper concludes in section 7.

2. Related Works

Literature survey revealed a wide spread application of Artificial Neural Networks in biometrics. However the application of SOFM in biometric seems to be scarce. Mai V et al [9] proposed a new method to identify people using Electrocardiogram (ECG). QRS complex (Q waves, R waves, S waves) which is a stable parameter against heart rate variability is used as a biometric feature. This work has reported for having achieved a classification accuracy of 97% using RBF.

Sulong et al [10] have used a combination of maximum

^{*} Corresponding author:

prashanthgk@sit.ac.in (Prashanth G. K.)

Published online at <http://journal.sapub.org/ajis>

Copyright © 2015 Scientific & Academic Publishing. All Rights Reserved

pressure exerted on the keyboard and the time latency between the keystrokes to recognize the authenticate users and to reject imposters. In this work, RBFNN is used as a pattern matching method. The system so developed has been evaluated using False Reject Rate (FRR) and False Accept Rate (FAR). The researchers have affirmed the effectiveness of the security system designed by them.

Chatterjee et al [11] have proposed a new biometric system which is based on four types of temporal postural signals. The system employs S-transform to determine the characteristic features for each human posture. An RBFNN with these characteristic features as input is developed for specific authentication. The training of the network has augmented extended Kalman filtering (EKF). The overall authentication accuracy of the system is reported to be of the order of 95%.

In a study, multi-modal biometric consisting of fingerprint images and finger vein patterns were used to identify the authorized users after determining the class of users by RBFNN as a classifier. The parameters of the RBFNN were optimized using BAT algorithm. The performance of RBFNN was found to be superior when compared with KNN, Naïve Bayesian and non-optimized RBFNN classifier [12].

Ankit Chadha et al have used signature of persons for verification and authentication purpose. RBFNN was trained with sample images in the database. The network successfully identified the original images with the recognition accuracy of 80% for image sample size of 200 [13].

Handwriting recognition with features such as aspect ratio, end points, junction, loop, and stroke direction were used for recognition of writers [14]. The system used over 500 text lines from 20 writers. RBFNN showed a recognition accuracy of 95.5% when compared to back propagation network.

Enhanced Password Authentication through Typing Biometrics with the KMeans Clustering Algorithm. [16]. Combination of supervised and unsupervised learning for clustering data without any preliminary assumption on the cluster shape is implemented for Iris dataset [17]. A new method directed towards the automatic clustering of x-ray images. The clustering has been done based on multi-level feature of given x-ray images such as global level, local level and pixel level. [18].

Suad K. Mohammad [19], have used a new method for Ear Recognition by Using Self Organizing Feature Map, They have developed and illustrated a recognition system for human ears using a Kohonen self-organizing map (SOM) or Self-Organizing Feature Map (SOFM) based retrieval system.

3. Kohonen's Feature Maps

The Self-Organising Map (SOFM) network performs unsupervised learning. It is neural network that forms

clusters that reflect similarities in the input vector. It is mapping that defined implicitly and not explicitly. This is desirable because this investigation is not restricted to any particular application or predefined categories. Input vector is presented sequentially in time without specifying the output. Because of the fact, there is no way of predicting which neurons will be associated with a given class of input vectors. This mapping is accomplished after training the network. The SOFM has sequential structure starting with the d input vector (input neurons) \mathbf{x} , which are received by the neurons in parallel and scaled by the weight vector \mathbf{w} . Thus the weight matrixes the size of neurons by d inputs. The n neurons are then entered into competition where only one neuron wins. This architecture of the SOFM is illustrated in Fig.1. SOFM employs the concept of topological neighbourhoods, which are equidistance neuron neighbourhoods centred around a particular neuron. The neighbourhood centred around a particular neuron. The neighbourhood distance matrix for a one-dimensional case using four neurons is:

0	1	2	3
1	0	1	2
2	1	0	1
3	2	1	0

It can be seen that the distance of neuron from itself is 0, the distance of neuron from its immediate neighbour is 1, and so on.

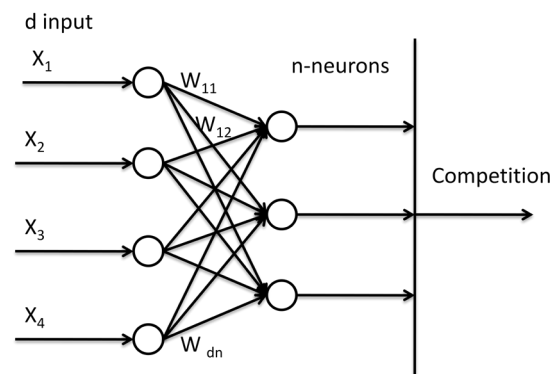


Figure 1. Architecture of Kohonen Feature Map

Unlike simple comparative learning, the weights of the neighbourhood neurons are updated in addition to the weights of the winning neuron. SOFM algorithm can be outlined as follows:

Step 1: Initialize weights randomly.

Step 2: Present new input.

Step 3: Compute distance between input and neuron weights.

Step 4: Competitive selection of the neurons with the minimum distance.

Step 5: Update neuron weights to winning neurons and neighbourhood neurons.

Step 6: Continue iterating by going through step 2-5.

In describing the training algorithm, it is useful to understand the weight structure of the network. Each neuron

has the same number of weights w as the dimension of the input vector x . The weight structure for each neuron can then be viewed as a matched filter competing against other neurons. A matched filter has the impulse response tuned to input so that it produces the maximal signal. w The overall, weight structure can be viewed as an array of matched filters with each neuron's weights being adjusted on the basis of current weights and the goodness-of-match of the input. Given that the feature map is initialized with random weights w for all the neurons, a distance measure, $d(x, w_i)$ can be used to define the goodness-of-match between a particular weight vector w_i and the input vector x . The distance measure used can be correlation, Euclidian, city-block, or other statistical measures. If the Euclidian distance is used, then the winning neuron from the competition is found at each iteration k by using the following equation:

$$\|x(k) - w_c(k)\| < \|x(k) - w_i(k)\| \quad (1)$$

where neuron c is the winning neuron. The network weights are then updated to $w_i(k+1)$ as follows:

$$w_i(k) + a(k)(x(k) - w_i(k)), i \in N_c(k) \\ w_i(k), i \notin N_c(k) \quad (2)$$

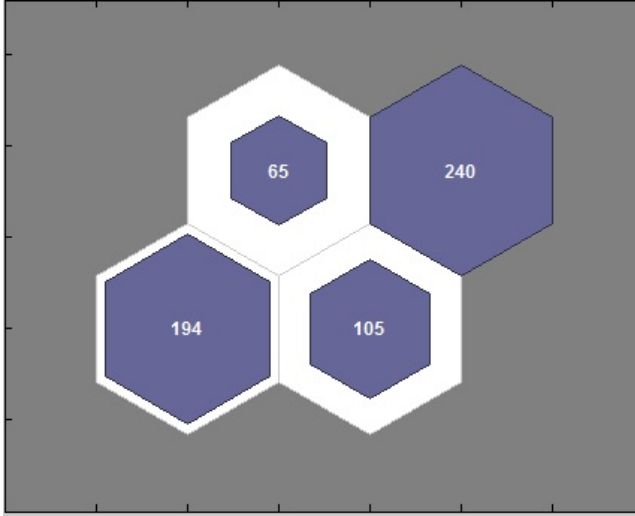


Figure 2. SOM Sample Hits

Where N_c defines the neuron neighbourhood and $a(k)$ is the learning rate at each iteration. The weight updating equation shows that $d(x, w_i)$ is decreased for N_c while those outside N_c are left unchanged. The neighbourhood size and the learning rate both decrease with increase in the number of training iterations. Typically, $a(k)$ start near 1 and go down to 0.1. The size N_0 can start out as large as the greatest distance between weight vectors, and decrease until the neighbourhood defines only one neuron. An interesting feature of SOFM is that the distances between neurons can be interpreted as statistical frequency distributions. In a fully trained network, if input vectors occur with varying frequencies, the feature map will also allocate neurons to an area in proportion to the frequency of input vectors. Another interesting feature of SOFM is that the weights become topologically similar to the input vectors. In a sense, the final

weights are analogous to class templates and can be plotted for visual interpretation. Because of this feature, the SOFM is less like a black box and more like an automated k-means statistical clustering algorithm.

The choice of the particular SOFM configuration is not a precise science and involves engineering judgment. The two major design parameters are dimension of the network and the number of neurons. Powerful results have been obtained by just using one and two-dimensional topologies. The training parameters are the learning rate and the number of training iterations. The initial learning rate may be between 0 and 1, and the value of 0.2 was chosen based on experience. Kohonen cites the use of 10,000-1,00,000 training iterations as typical, and recommends that the number of training cycles should be at least 500 times the number of output neurons.

3.1. SOM Sample Hits

SOM hits calculates the classes for each neuron and shows the number of neurons in each class. Areas of neurons with large numbers of hits indicate classes representing similar highly populated regions of the feature space. Whereas areas with few hits indicate sparsely populated regions of the feature space [20-24].

The default topology of the SOM is hexagonal. This figure shows the neuron locations in the topology, and indicates how many of the training data are associated with each of the neurons (cluster centres). The topology is a 2-by-2 grid, so there are 4 neurons. The maximum number of hits associated with any neuron is 240 and minimum is 65. In this work, 5x605 matrix is considered as input data. After clustering using SOFM 605 data were divided into 4 neurons (clusters). First neuron hit 194 times, second neuron hit by 105 times, third by 65 and forth by 240. Such sample and hits are shown in Figure 2.

3.2. SOM Topology

SOM training, the weight vector associated with each neuron moves to become the centre of a cluster of input vectors. In addition, neurons that are adjacent to each other in the topology should also move close to each other in the input space, therefore it is possible to visualize a high-dimensional inputs space in the two dimensions of the network topology. The default SOM topology is hexagonal [25].

3.3. SOM Neighbour Connection

SOM Neighbour Connection shows the SOM layer, with the neurons denoted as a dark patches and their connection with their direct neighbour denoted as line segment. Neighbour typically classify similar sample. [26]

3.4. SOM Neighbour Distance

SOM Neighbour weights distance shows to what extent (in terms of Euclidian distance) each neuron classes are from its neighbour. Connections which are bright indicate highly

connected areas of the input space. While dark connection indicates classes representing regions of the feature spaces which are far apart, with few or no neurons between them.

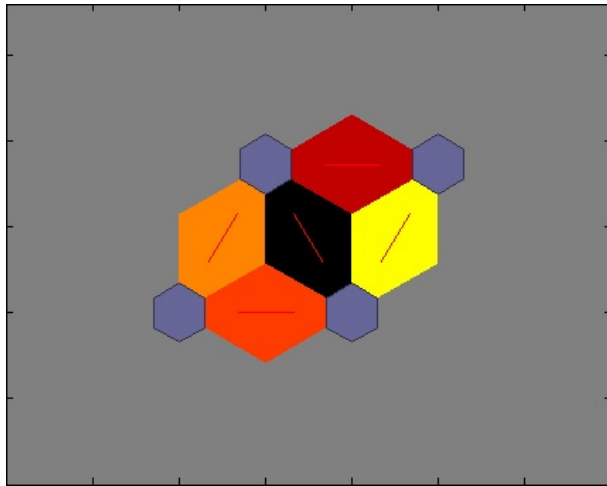


Figure 3. SOM Neighbour Distance

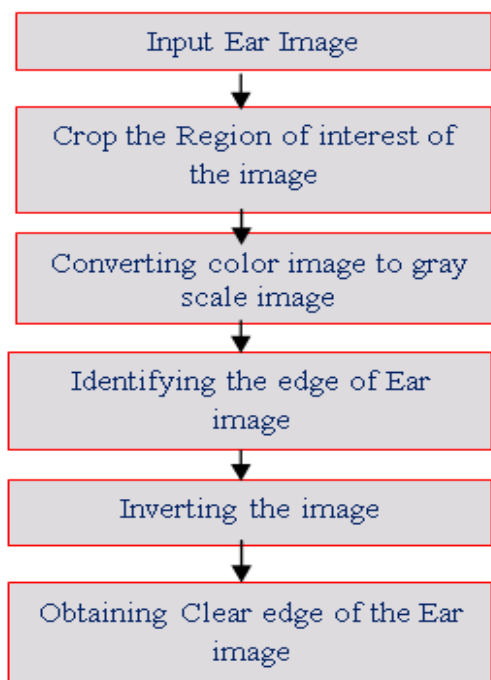


Figure 4. The Steps involved in ear edge extraction

Long borders of dark connection separating large regions of the input space indicates that the classes on either side of the border represents neurons with very different features. [23]

3.5. SOM Input Planes

SOM Plane shows a weight plane for each of the five input features. They are visualization of the weights that connected each input to each of the 4 neurons in the 4x4 hexagonal grid. Darker colour represents larger weights. If two inputs have similar weights planes (their colour gradients may be the same or in reverse) it indicates they are highly correlated.

4. Data Acquisition

The ear biometric recognition systems can also be divided into five main parts - image acquisition, pre-processing, feature extraction, extraction of feature vector and classification & comparison [3]. The process of ear edge extraction is shown in Figure 4. A typical edge of the ear is also shown in Figure 5.

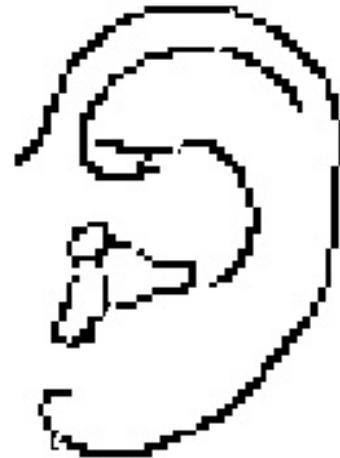


Figure 5. The Outer Edge of Ear (Typical)

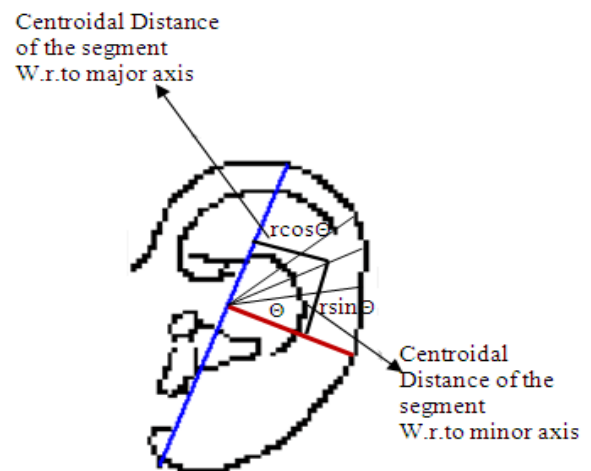


Figure 6. Segments of Ear

5. Feature Extraction

To start with, the major axis and minor axis were identified. Major axis is the one which has the longest distance between two points on the edge of the ear, the distance here is the maximum among point to point Euclidean distance. The minor axis is drawn in such way that it passes through tragus and is orthogonal to the major axis. Therefore, with different orientation of ears the orientation of major axis also changes. Being perpendicular to major axis, the orientation of minor axis is fixed.

The surface area of the ear is the projected area of the curved surface on a vertical plane. This area is assumed to be formed out of segments. Only the area of an ear to the right side of the major axis is considered to be made out of six segments. Each of the segments thus subtends 30° with respect to the point of the intersection of the major axis and minor axis. The extreme edge of a sector is assumed to be a circular arc. Thus converting each segment into a sector of a circle of varying area. One such typical segment is shown in figure and a measurement involved over such segment is presented in Figure 6.

The measurements are

- $\theta \rightarrow$ Inclination of the central radial axis of the segment with respect to minor axis (in degrees).
- $r \rightarrow$ The length of the radial axis (in mm).

The conversion of number of pixels into linear dimension (in mm) was based on the resolution of the camera expressed in PPI (Pixel Per Inch). In this work 16Mega pixel camera, at 300 PPI was used. The computation of linear distance is straight forward, ie $\text{mm} = (\text{number of pixel} \times 25.4) / \text{PPI}$ [1 inch=25.4 mm].

The moment of inertia with respect to major axis I_{\max} , x_i is the perpendicular distance of the centroid of the i th segment with respect to major axis. I_{\max} of the entire area is given by;

$$I_{\max} = \sum_{i=1}^6 a_i x_i^2 \quad (1)$$

Moment of inertia with respect to minor axis I_{\min}

$$I_{\min} = \sum_{i=1}^6 a_i y_i^2 \quad (2)$$

From the computed values of moment of inertia and area of the ear surface, the radii of gyration with respect to minor axis(RGx)and major axis(RGy) were computed. The formulae for radii of gyration are given by[27].

$$RGx = \sqrt{\frac{I_{\min}}{A}} \quad (3)$$

$$RGy = \sqrt{\frac{I_{\max}}{A}} \quad (4)$$

Where, A is the sum of areas of six segments. Including Major axis and minor axis.

$$A = \sum_{i=1}^6 a_i \quad (5)$$

5.1. Shape Based Biometrics

The five shape based features of ears that were considered for classification are listed in the Table 1. The details of feature extraction and their evaluation authentication and validation are available in seminal work of authors [27]. However, for the sake of clarity, the features are briefly explained in the following paragraphs.

The surface area of the ear is the projected area of the curved surface on a vertical plane. Moment of Inertia (MI) is the property of a planar surface which originates whenever one has to compute the moment of distributed load that varies linearly from the moment axis. Radii of gyration is the distance from an axis at which the mass of a body may be assumed to be concentrated and at which the moment of inertia will be equal to the moment of inertia of the actual mass about the axis. It is also equal to the square root of the quotient of the moment of inertia and the mass.

Table 1. Shape based features for classification

Sl. No	Attributes
1	Area
2	Moment of Inertia Y (I_{\max})
3	Radii of gyration Y (RGy)
4	Moment of Inertia X (I_{\min})
5	Radii of gyration X (RGx)

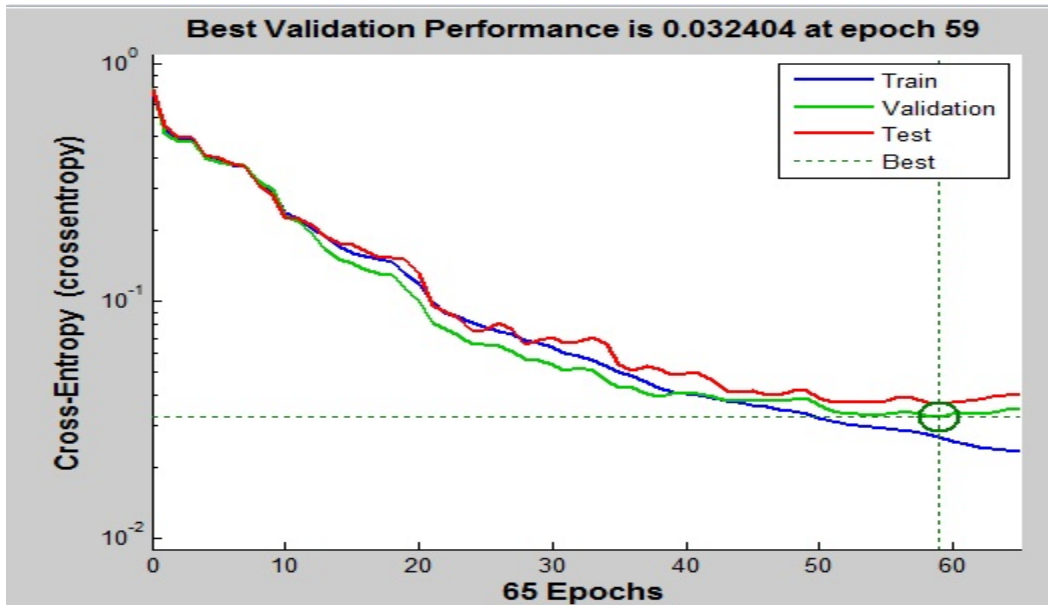


Figure 7. The Mean Square Error

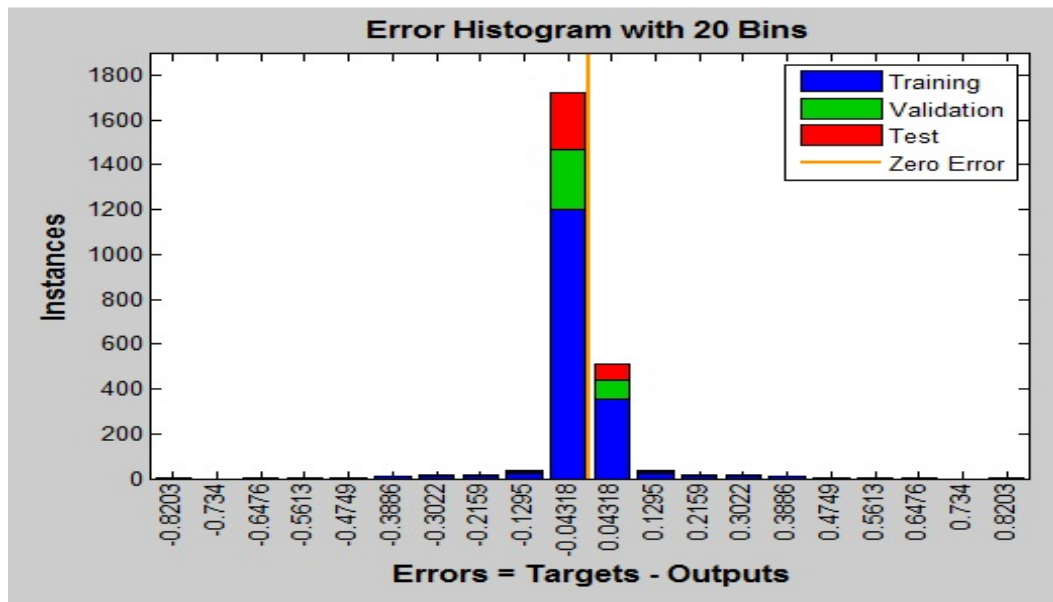


Figure 8. Error Histogram

6. Result and Discussion

Table 2 shows the sample database used for this work. From Figure 7, it is evident that the errors involved during validation are at lower level when compared to errors that happened during training. The histogram is indicative of the fact the low errors in the range of -0.04318 and 0.04318 for most of the samples. The training errors are also to the tune of 0.0886 which is very low.

Confusion matrix pertaining to classification is shown in Figure 9. From the matrix it is clear that the overall correctly classified ear images stands at 98.8%.

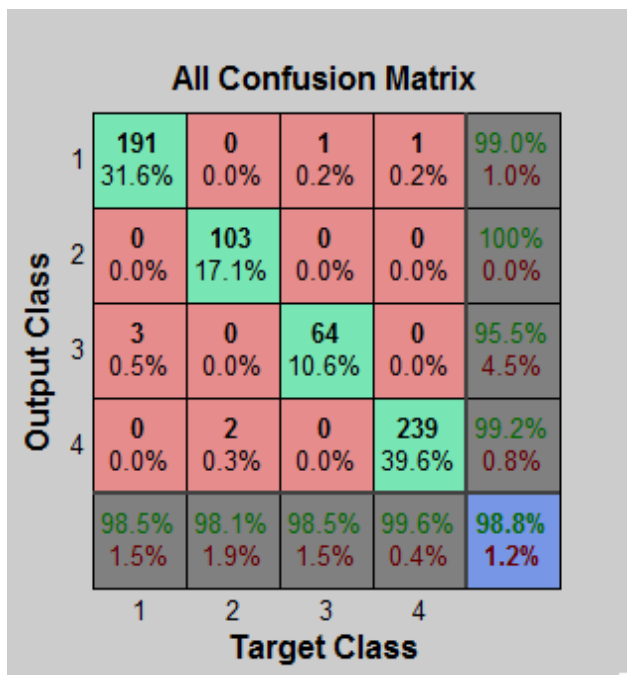


Figure 9. Confusion Matrix

After the classification task, the data base was studied to elicit the characteristic features of the groups. This information is presented in Table 3.

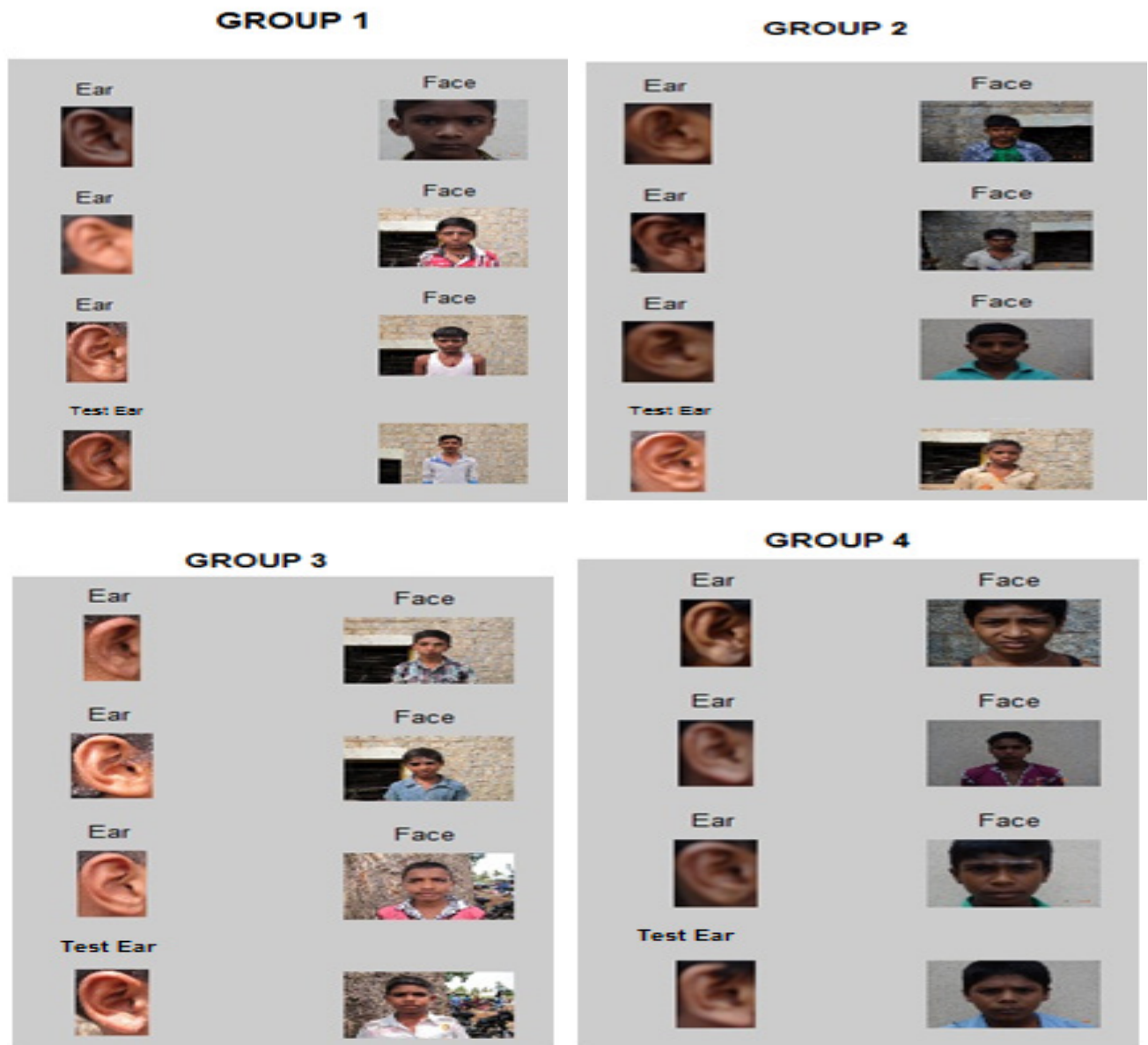
Figure 10 shows the test image and a few members of the same group.

Table 2. Test Set and Group Indexing By SOFM

Area	Imax	Rgy	Imin	RGx	GI
200.0225	5604194	167.3852	13.5314	0.260095	C4
234.6544	1589893	82.31322	68.01732	0.538388	C2
208.4046	615617.2	54.35027	109.5619	0.725064	C2
381.0366	4705829	111.1309	233.138	0.78221	C4
419.6705	3784483	94.96183	152.9465	0.603692	C2
235.727	852258.8	60.1286	579.94	1.568509	C1
404.4997	3315528	90.53515	27.28417	0.259715	C4
295.0065	2720260	96.02614	6.276003	0.145857	C1
328.0722	3792994	107.5242	22.80077	0.263627	C4
349.374	4835772	117.6488	3.869048	0.105234	C4
413.2613	4095080	99.54485	1094.115	1.627118	C4
250.2391	1797717	84.75845	194.1038	0.880723	C4
327.1153	4167137	112.8674	91.37789	0.528531	C1
421.2443	4775864	106.4778	905.9184	1.466485	C1
228.3155	2882784	112.3669	1.643953	0.084855	C1
160.6659	1647154	101.2524	22.7681	0.376445	C3
341.1719	1767501	71.97691	645.0942	1.375071	C1
195.1159	1451804	86.25965	51.07464	0.51163	C4
323.5646	1830669	75.21845	686.2381	1.45632	C1
318.7034	2038488	79.97619	516.502	1.273042	C3
322.2193	1663035	71.84143	582.7104	1.344778	C1
367.059	2755478	86.64242	575.4669	1.252109	C3
535.4865	6017210	106.0043	2150.653	2.004061	C3
416.0734	3387038	90.22462	1315.284	1.777972	C4

Table 3. Group Characteristics

Group Index	Area (mm ²)	Imax (mm ⁴)	RGy (mm)	Imin (mm ⁴)	RGx (mm)	Approximate shape
1	99.46609	16329.43	8.960133	0.039619	0.009685	Almost Round, oblong
	647.7786	14331267	148.7404	3893.686	2.702608	
2	79.676	130778.9	21.19714	0.344449	0.035572	attach lobe to the side of the face oval arc elliptical shape
	689.8224	10722679	156.1173	3243.304	2.295692	
3	81.16401	90537.02	29.86013	0.403941	0.048645	border lobe almost square or rectangular shape
	543.1691	7402272	169.5496	2150.653	2.004061	
4	85.89321	95414.44	32.45999	0.000004	0.000121	fanned out and pointed ear with rectangular shape at the top
	834.7111	13888527	177.1114	7720.38	3.920185	

**Figure 10.** Test images and a small segment of the corresponding Group

7. Conclusions

This paper presented SOFM based image matching and personal identification. SOFM provided four subset of ears with typical characteristic features. To effectively utilize SOFM generated groups the matching of test ear images was done on ear image database which was organised as per groups. This resulted in reduction of CPU time for matching and retrieval of images to an extent of 10% when compared with the time taken for matching and retrieval of the same in unorganised ear database.

REFERENCES

- [1] Abate, A. F., Nappi, M., Riccio, D., & Ricciardi, S. 2006. Ear recognition by means of a rotation invariant descriptor. In International Conference on Pattern Recognition, 437–440.
- [2] Abdel-Mottaleb, M., & Zhou, J. 2005. Human ear recognition from face profile images. In ICB, 786–792.
- [3] Abdel-Mottaleb, M., & Zhou, J. 2006. Human ear recognition from face profile images. In ICB, 786–792.
- [4] Sukhdeep Singh, Dr. Sunil Kumar Singla, "A Review on Biometrics and Ear Recognition Techniques", Singh et al., International Journal of Advanced Research in Computer Science and Software Engineering 3(6), June - 2013, pp. 1624-1630.
- [5] Cunnings; A.H.; Nixon, M.S.; Carter; JN, "Anovel ray analogy for enrollment for earbiometrics", IEEE 2010
- [6] DJ. Hurley, M.S. Nixon, I. N. Carter, "Force field feature extraction for ear biometrics", Computer vision and image understanding, Vol. 98, No. 3, pp.491-512, 2005.
- [7] B. Victor, K. Bowyer, and S. Sarkar, "An Evaluation of face and Ear Biometric", 16th International conference of Pattern Recognition, pp.429-432, 2002.
- [8] K. Chang, K.Bowyer, and V. Barnabas, "Comparison and Combination of Ear and Face Image in Appearance-Based Biometrics", IEEE Transactions on Pattern Analysis and Machine Intelligence, Vol. 25, pp. 1160-1165, 2003.
- [9] Mai V, Khalil I, Meli C, "ECG biometric using multilayer perceptron and radial basis function neural networks", 33rd Annual International Conference of the IEEE EMBS Boston, Massachusetts USA, August 30 - September 3, 2011.
- [10] A. Sulong, Wahyudi and M.D. Siddiqi, "Intelligent Keystroke Pressure-Based Typing Biometrics Authentication System Using Radial Basis Function Network", 2009 5th International Colloquium on Signal Processing & Its Applications (CSPA).
- [11] Chatterjee, A., Fournier, R., Nait-Ali, A., Siarry, P., "A Postural Information-Based Biometric Authentication System Employing S-Transform, Radial Basis Function Network, and Extended Kalman Filtering", Instrumentation and Measurement, IEEE Transactions on Volume:59, Issue: 12.
- [12] Anand Viswanathan, S. Chitra, "Optimized Radial Basis Function Classifier for Multi Modal Biometrics", Research Journal of Applied Sciences, Engineering and Technology 8(4): 521-529, 2014 ISSN: 2040-7459; e-ISSN: 2040-7467.
- [13] Ankit Chadha, Neha Satam, Vibha Wali, "Biometric Signature Processing & Recognition Using Radial Basis Function Network", CiiT International Journal of Digital Image Processing, ISSN 0974 – 9675 (Print) & ISSN 0974 – 956X (Online) September 2013.
- [14] Ashok. J, Rajan. E.G, (2010) "Writer Identification and Recognition Using Radial Basis Function", Int. Jour. of Computer Science and Information Technologies, 1(2), 51-57.
- [15] Kunte. R.S and Samuel. R.D.S, (2007) "A simple and efficient optical character recognition system for basic symbols in printed Kannada text", SADHANA, 32(5), 521–533.
- [16] Cheng Soon Ong and Weng Kin Lai, "Enhanced Password Authentication through Typing Biometrics with the KMeans Clustering Algorithm," Proc. Of Seventh International Symposium on Manufacturing with Applications (World Automation Congress), Maui, Hawaii, June 11-16, 2000.
- [17] Satish R. Kolhe, Ranjana S. Zinjore "Clustering Iris Data using Supervised and Unsupervised Learning.", International Journal of Computer Science and Application Issue 2010, ISSN 0974-0767.
- [18] Chhanda Ray, Krishnendu Sasmal "A New Approach for Clustering of X-ray Images". IJCSI International Journal of Computer Science Issues, Vol. 7, Issue 4, No 8, July 2010 ISSN (Online): 1694-0784 ISSN (Print): 1694-0814
- [19] Suad K. Mohammad, Ear Recognition by Using Self Organizing Feature Map, Eng. & Tech. Journal, Vol. 31, Part (A), No.10, 2013
- [20] Jamil Ahnad, M. and G.N. Tiwari. 2009. Optimization of tilt angle for Solar Collector to receive Maximum Radiation" The Open Renewable Energy Journal, 2: 19-24.
- [21] Sundarraj, M., 2013. Study Of Compact Ventilator, Middle-East Journal of Scientific Research, ISSN:1990-9233, 16(12): 1741-1743.
- [22] Sundar Raj, M., T. Saravanan and R. Udayakumar, 2013. Energy Conservation Protocol for Real time traffic in wireless sensor networks, Middle-East Journal of Scientific Research, ISSN:1990-9233, 15(12): 1822-1829.
- [23] Sundar Raj, M. and T.R. Vasuki, 2013. Automated Anesthesia Controlling System, Middle-East Journal of ScientificRes., ISSN:1990-9233, 15(12): 1719-1723.
- [24] Sundar Raj, M., T. Saravanan and R. Udayakumar, 2013. Data Acquisition System based on CAN bus Subspace-based facerecognition in analog VLSI," in and Research, ISSN:1990-9233, 15(12): 1857-1860.
- [25] M.C. Nataraja, M.A. Jayaram, C.N. Ravi Kumar, "Kohonens Feature Maps for Fly Ash Catgorization", world scientific, International Journal of Neural System, vol 6, no 6, 2006.
- [26] Bhanu and H. Chen, B. "Human ear recognition in 3D", In Workshop on Multimodal User Authentication, pages 91–98, 2003.
- [27] M.A. JAYARAM, Prashanth G.K., Sachin C Patil, Inertia Based Ear Biometrics: A Novel Approach, Journal of

Intelligent systems, 2015.

- [28] Egor P Popov, Engineering mechanics of solids, Easter Economy Edition, 2nd edition, 1998.
- [29] Braja M. Das, Paul C. Hassler, Statics and Mechanics of materials, Prentice Hall, 1988.